Accepted author manuscript, published in final form in Rapid Commun. Mass Spectrom. 28, 1144-1152

Identification and significance of unsaturated archaeal tetraether lipids in marine sediments

Chun Zhu*, Marcos Y. Yoshinaga, Carl A. Peters[1], Xiao-Lei Liu, Marcus Elvert, Kai-Uwe Hinrichs

MARUM Center for Marine Environmental Sciences and Department of Geosciences, University of Bremen, D-28359 Bremen, Germany

[1]current address: Department of Earth and Planetary Sciences, Macquarie University, Sydney, NSW 2109, Australia

*corresponding author: czhu@uni-bremen.de

Running head: unsaturated archaeal tetraether lipids

Abstract

RATIONALE: Studies of archaeal glycerol dibiphytanyl glycerol tetraethers (GDGTs) in the environment and cultures have exclusively focused on compounds with fully saturated alkyl moieties. Here we report a number of novel unsaturated GDGTs (uns-GDGTs) whose alkyl chains contain up to six double bonds and zero to two cyclopentyl moieties.

METHODS: The identification of these lipids was achieved via comparison of lipid distribution before and after hydrogenation, characteristic retention time patterns, and diagnostic fragments using liquid chromatography/mass spectrometry (LC/MS), and ether cleavage products using gas chromatography/mass spectrometry (GC/MS). Isomerism resulting from different unsaturation patterns in the alkyl moieties was observed and specific positions of double bonds in the biphytene and biphytadiene moieties were tentatively assigned.

RESULTS: Uns-GDGTs were detected in sediment and microbial mat samples as both core lipids (CLs) and intact polar lipids (IPLs) associated with mono- or diglycosyl or phosphatidylglycerol headgroups. However, these lipids were overlooked in past investigations because conventional methods for archaeal lipid analysis are unsuitable for uns-GDGTs. Samples from distinct marine environments (Black Sea, Cariaco Basin, Discovery Basin, Eastern Mediterranean Sea, upwelling area off NW Africa, and seep sites off Crimea and Pakistan) were screened for uns-GDGTs using a recently introduced LC/MS protocol. The results show that uns-GDGTs contribute significantly to the archaeal lipid pool in anoxic methane-rich environments (Black Sea, Cariaco Basin, and both seep sites) but they were barely detected in the oxic and hypersaline settings.

CONCLUSIONS: The characteristic distribution of uns-GDGTs implies that they are attractive targets for future studies aiming at chemotaxonomy of uncultivated archaea and regulation of uns-GDGT biosynthesis.

Key words: unsaturated GDGTs, membrane lipids, archaea, cold seeps, microbial mats, euxinic basins

Introduction

Archaea, the third domain of life, occupy a wide range of marine and terrestrial environments and possess diverse membrane lipids that adapt to different growth conditions (e.g., [1; 2]). Among archaeal membrane lipids, double bonds have been frequently reported in diphytanyl glycerol diethers (DGDs, e.g., archaeols) and isoprenoidal hydrocarbons (e.g., crocetenes and pentamethylicosenes) found in cultured halophiles [3; 4] thermophiles [5], methanogens [6; 7], and environmental samples of uncultured anaerobic methanotrophs [8-11], all of which belong to the Euryarchaeota. The proportion of unsaturated DGDs (uns-DGDs) increases with increasing ambient NaCl concentration in cultured halophilic archaea [4], and with decreasing growth temperature in cultured psychrophilic archaea [12-14; 3], indicating that biosynthesis of uns-DGDs represents a phenotypic adaptation. However, the physiological role of unsaturated archaeal isoprenoidal hydrocarbons remains unclear.

Although representing a dominant lipid class in the vast majority of archaea, glycerol dibiphytanyl glycerol tetraethers (GDGTs) are generally considered to consist exclusively of saturated alkyl moieties. However, *Archaea* are capable of modifying the saturated biphytanyl moieties of GDGTs in a variety of ways to cope with environmental stress, including cyclization, methylation, and hydroxylation of biphytanyl moieties, and formation of a covalent bond between two biphytane skeletons [15; 2; 16; 17]. By analogy to the existence of uns-DGDs, incorporation of double bonds into the alkyl moieties of GDGTs appears to be a feasible adaptive response. Nevertheless, unsaturated GDGTs (uns-GDGTs) have not been reported so far.

Here, we report previously unidentified uns-GDGTs with one to six double bonds in marine sediments; their detection is facilitated by a recently introduced analytical protocol [18]. An initial

survey of uns-GDGTs in several distinct marine environments reveals their significance in seep sites and euxinic basins.

Materials and methodology

The sample set and biogeochemical regimes.

Our sample set covers distinct marine environments (Table 1) with different water chemistry, availability of organic substrates, and potential energy supply by biogeochemical processes. In brief, i) a microbial mat sample from chimney-like buildups was taken from an active Crimean seep in the GHOSTDABS field, NW Black Sea, where massive microbial mats are typical associated with methane-derived carbonates [19]. Sediment samples were collected from ii) a cold seep site off Pakistan, in which focused upward migration of methane stimulates high rates of anaerobic oxidation of methane (AOM) [20]; iii) the Black Sea and iv) Cariaco Basin - despite reduced fluxes relative to seep sites, methane is also released from the seafloor and accumulates in the overlying anoxic water column of these two anoxic basins [21]; v) the Eastern Mediterranean Sea, a well-ventilated oligotrophic sea with an oxic seafloor since the deposition of the most recent sapropel [22]; vi) an upwelling area off northwest Africa characterized by high primary productivity, extensive degradation of organic matter, the continuous presence of oxygen throughout the water column, and oxic sediments on the top of the seafloor (WOA09); and vii) the hypersaline Discovery Basin in the eastern Mediterranean Sea with extremely high concentrations of Mg^{2+} and Cl^{-} [23].

Sample preparation

Lipids were extracted from freeze-dried and homogenized sediments by either Soxhlet (sediments form the Black Sea, Cariaco Basin, and off NW Africa) [21] or a modified Bligh and Dyer protocol [24] (Table 1). The hydrogenation experiment was based on Schouten et. al (2007) [25] with modifications. In brief, an aliquot of the total lipid extract (TLE) was dissolved in ethyl acetate containing 100 mg of platinum oxide and 100 µL of acetic acid. The samples were hydrogenated by flushing with H_2 at room temperature for 20 min and subsequently sealed and maintained at 60°C for 3 h. Aliquots before and after hydrogenation were analyzed by liquid chromatography/mass spectrometry (LC/MS) for uns-GDGTs, respectively.

Another aliquot of the TLE was used for archaeal lipid purification [26], and the diglycosidic tetraether fraction, containing 85% of diglycosidic uns-GDGTs (data not shown), was subjected to ether cleavage reaction with BBr_3 and subsequent lithiumtriethylboronhydride (superhydride; Sigma-Aldrich, Steinheim, Germany) reduction as described by Jahnke et al. (2008) [27]. The resultant hydrocarbons were analyzed by gas chromatography/mass spectrometry (GC/MS).

Instrumentation

LC/MS

Reverse phase (RP) liquid chromatography/electrospray ionization/mass spectrometry (RP-LC/ESI/MS) was performed on an Agilent 1200 series HPLC system coupled to an Agilent 6130 MSD single quadrupole mass spectrometer (Agilent Technologies, Waldbronn, Germany) operated in full scan mode (*m/z* 500-2000; positive mode) via an ESI interface (RP-LC/ESI/MS_{MSD}). The optimum conditions of ESI/MS_{MSD} were: capillary voltage 4000 V, nebulizing gas (N_2) pressure 4.14 bar (60 psi), dry gas (N_2) 5 ml/min at a temperature of 200 °C, vaporizer temperature 150 °C, and fragmentor voltage 180 V. In order to confirm uns-GDGTs

through accurate masses and diagnostic product ions, selective samples were also analyzed using a Dionex Ultimate 3000 UHPLC system coupled to a Bruker maXis Ultra-High Resolution orthogonal accelerated quadrupole-time-of-flight (qTOF) tandem MS via an ESI interface (RP-LC/ESI/MS_{qTOF}), where uns-GDGTs were targeted for MS/MS (MS^2) fragmentation in a multiple reaction monitoring (MRM) mode. The optimum conditions of ESI/MS_{qTOF} and its mass calibration were based on the method introduced by Zhu et al. (2013) [18]. Both RP-LC/ESI/MS_{MSD} and RP-LC/ESI/MS_{qTOF} analyses were performed under identical LC conditions as described in Zhu et al. (2013) [18]. Briefly, the RP chromatographic separation of ether lipid mixtures (dissolved in methanol prior to injection) was achieved on an ACE3 C_{18} column (3 µm, 2.1 × 150 mm; Advanced Chromatography Technologies Ltd., Aberdeen, Scotland) coupled with a guard cartridge and maintained at 45 °C. Ether lipids are eluted isocratically with 100% A for 10 min, followed by a rapid gradient to 24% B over 5 min, and then a slow gradient to 65% B over another 55 min at a flow rate of 0.2 mL/min, where the eluent A is 100:0.04:0.10 of methanol/formic acid/14.8 M NH_3(aq.) and B is 100:0.04:0.10 of 2-propanol/formic acid/14.8 M NH_3(aq.). The column is washed with 90% B for 10 min and subsequently re-equilibrated with 100% A for another 10 min before the next injection. Lipids were detected as $[M+NH_4]^+$ with ESI/MS analysis.

Normal phase liquid chromatography/atmospheric pressure chemical ionization/MS (NP-LC/APCI/MS) analysis of core GDGTs was based on the method described by Schouten et al. (2007) [28] and implemented on an Agilent 1200 series HPLC system coupled to an Agilent 6130 MSD via a multimode interface set to APCI mode (NP-LC/APCI/MS_{MSD}). In brief, separation of core GDGTs was achieved on a Prevail Cyano (CN) column (150 mm × 2.1 mm, 3 µm; Alltech; Deerfield, IL, USA) maintained at 30°C. Core GDGTs were eluted isocratically with 100% A for

5 min, followed by a linear gradient to 9% B over 45 min, where A is hexane: 2-propanol (99:1, v/v) and B is hexane: 2-propanol (90:10, v/v) at a flow rate of 0.2 mL/min. APCI/MS_{MSD} conditions were optimized according to Zhu et al. (2013) [18]. Lipids were detected as $[M+H]^+$ with APCI/MS analysis in full scan (*m/z* 500-1500) mode.

The impact of ionization mode of NP-LC/APCI/MS_{MSD} on the detection of uns-GDGTs was evaluated by changing the interface to ESI while keeping the fragmentor voltage and LC conditions constant on the same instrument (i.e., NP-LC/ESI/MS_{MSD}). Post column buffers (100:0.12:0.04 of 2-propanol/formic acid/14.8 M NH_3) were added via T-piece to assist electrospray ionization.

GC/MS

GC/MS analysis for biphytanes and biphytenes derived from ether cleavage experiments was performed on a Trace Gas Chromatograph/electron ionization/MS system (ThermoFinnigan, San Jose, CA, USA) operated in positive mode. The GC injector temperature was 310 °C in split/splitless mode and separation was achieved on a Restek Rxi-5ms column (30 m × 250 μm × 0.25 μm, Restek, Bad Homburg, Germany). The GC was programmed to an oven temperature program of 60 °C (hold for 1 min) to 150 °C at 10 C min^{-1} and then to 310 °C (held 20 min) at 4 °C min^{-1}.

Results and discussion

Identification of uns-GDGTs

RP-LC/ESI/MS_{MSD} analysis of a cold seep sediment off Pakistan detected saturated GDGTs with 0-4 cyclopentyl moieties ($GDGT_{0-4}$), crenarchaeol (cren) and its regioisomer (cren'), and

their intact polar lipid (IPL) counterparts. Notably, there are a number of additional ions of *m/z* 1317.3 (**I**), 1315.3 (**II** and **V**), 1313.3 (**III** and **VI**), and 1311.3 (**IV** and **VII**) (Fig.1A). These masses appear to be identical to the masses of ammoniated $GDGT_{1\text{-}4}$ molecules (i.e., *m/z* 1317.3, 1315.3, 1313.3, 1311.3). Accurate mass measurements using RP-LC/ESI/MS_{qTOF} subsequently confirmed that formulas of compounds **I-VII** are identical to those of ammoniated $GDGT_{1\text{-}4}$ (typically better than 2 ppm), suggesting the possible presence of double bonds and/or other cyclic moieties in GDGTs. We further performed a hydrogenation experiment, after which **I-VII** were not detected and only $GDGT_0$ and GDGTs with cycloalkylated biphytanyl moieties persisted (Fig.1B), indicating that **I-VII** are all unsaturated compounds. In order to examine the transformation of **I-VII** to their saturated counterparts after hydrogenation, the abundances of each tetraether was normalized to crenarchaeol (whose unsaturated counterparts were not detected) in each run. The results show a drastic increase in the crenarchaeol-normalized abundance of $GDGT_0$ (i.e., $GDGT_0$/crenarchaeol) from 0.40 before hydrogenation to 1.56 after hydrogenation and a moderated increase in $GDGT_1$ from 0.12 to 0.28; whereas others show minimal changes in relative abundances (Fig.1C). This change suggests a major fraction of **I-VII** has been transformed to $GDGT_0$, and a minor fraction to $GDGT_1$. It is known that during reverse phase chromatography, progressive addition of double bonds to a bacterial fatty acid [29] or an archaeal diether [18] results in a staircase-like decrease in retention time. By analogy, increase in the number of double bonds of a tetraether lipid would also progressively reduce its retention time. We observe two staircase-patterns in retention time, ranging from $GDGT_0$ to **IV** and from $GDGT_1$ to **VII** (dashed lines, Fig.1A), likely indicating that **I-IV** are $GDGT_0$ with one to four double bonds ($GDGT_{0:[1\text{-}4]}$) and **V-VII** are $GDGT_1$ with one to three double bonds ($GDGT_{1:[1\text{-}3]}$). These assignments are consistent with the relative abundance changes before and after

hydrogenation. Assuming comparable MS responses, the total abundance of **I-IV** ($GDGT_{0:[1-4]}$) is much higher than that of $GDGT_0$, resulting in a drastic increase in the relative abundance of $GDGT_0$ (from 0.40 to 1.56) after hydrogenation. In contrast, the total abundance of **V-VII** ($GDGT_{1:[1-3]}$) is comparable to that of $GDGT_1$, resulting in a moderate increase in the relative abundance of $GDGT_1$ (from 0.12 to 0.28) upon transformation (Fig.1C).

The existence of uns-GDGTs was further confirmed by LC/MS^2 experiments. The MS^2 spectrum of $[GDGT_0 + NH_4]^+$ (*m/z* 1319) displays two diagnostic product ions of *m/z* 743 and 557, representing the neutral loss of an acyclic biphytanyl (BP_0) moiety [30-32]. Likewise, product ions of *m/z* 743 and 555 from **I** ($[GDGT_{0:1} + NH_4]^+$; *m/z* 1317) are derived from a neutral loss of the BP_0 moiety (Fig. 2A). For **II** ($[GDGT_{0:2} + NH_4]^+$; *m/z* 1315), product ions of *m/z* 743, 557, and 555 (Fig. 2A) are generated, indicating two co-eluting isomers. While the *m/z* 743 and 557 ions result from dissociation of the acyclic di-unsaturated biphytenyl ($BP_{0:2}$) and BP_0 moieties that suggest a combination of BP_0 and $BP_{0:2}$, the *m/z* 555 represents a mono-unsaturated biphytenyl moiety ($BP_{0:1}$) and therefore indicates the alternative combination of two $BP_{0:1}$ moieties. Similarly, the MS^2 spectrum of **III** $[GDGT_{0:3} + NH_4]^+$; *m/z* 1313; Fig. 2A) indicates two co-eluting isomers with combinations of $[BP_{0:1} + BP_{0:2}]$ and $[BP_0 + BP_{0:3}]$, respectively, and this spectrum is almost identical to **VI** ($[GDGT_{1:2} + NH_4]^+$; *m/z* 1313; data not shown). Poly-unsaturated product ions are commonly present in very low abundance in the MS^2 spectra, presumably because they are unstable and subject to further fragmentation. However, attempts to further assign the specific double bond locations were hampered by high signal-to-noise ratios of highly fragmented product ions (*m/z* < 500) and unknown fragmentation patterns of the biphytenyl chains. The MS^2 spectra of the remaining **IV**, **V**, and **VII** are noisy due to their low abundances in our samples but they also show typical GDGT-like fragmentation patterns (data

not shown). Based on the evidence from accurate masses, hydrogenation, retention time profiles, and MS^2 spectra, we tentatively assigned **I-IV** to $[GDGT_{0:[1-4]} + NH_4]^+$ and **V-VII** to $[GDGT_{1:[1-3]} + NH_4]^+$

A purified fraction dominated by di-glycosyl-$GDGT_{0:[1-3]}$ was subjected to ether cleavage and the hydrocarbon products were analyzed by GC/MS analysis (Fig. 2B). Based on published mass spectra [33], saturated acyclic (BP_0) and mono- to tri-cyclic biphytanes (BP_{1-3}) were readily recognized. Eluting between BP_0 and BP_1, a series of isoprenoidal hydrocarbon compounds was observed, tentatively identified as acyclic biphytenes and biphytadienes with molecular ions of *m/z* 560 and 558 ($BP_{0:1}$ and $BP_{0:2}$, respectively; Fig. 2B). This is supported by their elution pattern following BP_0, which is in accordance to the elution pattern of similar unsaturated isoprenoidal hydrocarbons such as crocetenes or pentamethylicosenes [34; 8; 35]. Identification based on the molecular masses and retention behavior is reinforced by specific fragment ions. Compared with isobaric cyclic biphytanes, mass spectra of $BP_{0:1}$ and $BP_{0:2}$ display lower intensities of fragment ions *m/z* 165 and 195, which are attributed to the presence of cyclopentane moieties in BP_1 and BP_2 [33]. We cannot unambiguously determine the double bond positions in $BP_{0:1}$ and $BP_{0:2}$ without authentic standards, however, we tentatively assigned one double bond position at carbon atom 3 for the both compounds based on their common fragment ions of *m/z* 55, 69, and 83 (Fig. 2B). Since hydrocarbons associated with allylic ether bonds (i.e., a double bond at carbon atom 2) are subject to degradation during BBr_3-based ether cleavage [36], the recovery of hydrocarbons after BBr_3 treatment consistently suggests their derivation from non-allylic ethers. Accordingly, we suggest that the presence of uns-GDGTs bearing allylic ether bonds is responsible for the lower yield of unsaturated biphytanes obtained after ether cleavage when compared to the relatively high abundance of unsaturated GDGTs during LC/MS analysis.

The other double bond in $BP_{0:2}$ is likely located between C-7 and 15 based on the fragment ions of *m/z* 111 and 123 (cf. [36]).

Uns-GDGTs also occurred as intact polar lipids (IPLs), the biological precursors of core lipids (CLs) in the samples (Fig. 3). Specific headgroups of IPL-uns-GDGTs were identified through diagnostic neutral losses [24] and accurate masses; the detected headgroups in the current sample set included mono- and di-glycosyl-, and phosphatidylglycerol (1G, 2G, PG, respectively) associated with either unsaturated-acyclic- or unsaturated-cyclic-GDGT core moieties. By contrast, unsaturated crenarchaeols, either CLs or IPLs, were not detected.

Despite their significance (Fig. 4A) in, for example, the cold seep sediment, uns-GDGTs were barely detected using the common NP-LC/APCI/MS approach [28] (Fig. 4B). This is attributed to the co-elution of uns-GDGTs and their isobaric, cyclic GDGTs (Fig. 4A vs. B) during NP chromatography, and subsequently in-source fragmentation of uns-GDGTs during APCI (Fig. 4B vs. C). This limitation of NP-LC/APCI/MS_{MSD} analysis is illustrated by $GDGT_{0:2}$: a strong fragment ion of *m/z* 743 co-occurs with a molecular ion of *m/z* 1298 in full-scan mode without collision-induced dissociation (Fig. 4B). However, once the APCI mode was replaced by ESI (i.e., NP-LC/ESI/MS_{MSD}), the *m/z* 743 ion was not detected while the signal of the *m/z* 1298 ion was greatly enhanced (Fig. 4C), indicating that the commonly used NP-LC/APCI/MS approach is inappropriate for the analysis of uns-GDGTs.

Environmental significance of uns-GDGTs

The methane index (MI) defines the ratio of cyclic $GDGT_{1-3}$ against crenarchaeol and its regioisomer as an index sensitive to methane oxidation mediated by archaea [37]. A MI value > 0.5 is suggestive of methane-charged sediments and 0.3-0.5 marks the boundary between normal

248 marine sediments and methane-rich sediments [37]. However, the recognition of uns-GDGTs in
249 environmental samples likely complicates the use of this proxy based on NP-LC/APCI/MS
250 measurements. For example, in our study, lipid analysis of the cold seep sediment off Pakistan
251 yielded different MI values (0.35, 0.50, 0.72; Fig. 4D) by the three analytical protocols (RP-
252 LC/ESI/MS, NP-LC/APCI/MS, and NP-LC/ESI/MS). NP-LC/APCI/MS and NP-LC/ESI/MS
253 measurements yielded apparently higher values, likely resulting from the contributions of co-
254 eluting uns-GDGTs to the peaks of $GDGT_{1-3}$. By contrast, RP/ESI/MS [18] resulted in a MI value
255 of 0.35 for the investigated cold seep site, which is still above the threshold value (i.e., 0.3) of
256 methane impact, but much lower than those reported for methane-rich environments [37]. This
257 suggests that in addition to $GDGT_{1-3}$, co-eluted uns-GDGTs are also responsible for elevated MI
258 values after NP lipid chromatography. Consequently, a readjustment and fine-tuning of the MI
259 using the RP-LC/ESI/MS protocol seems reasonable.

260 We further examined the environmental distribution of uns-GDGTs in samples from
261 geochemically and oceanographically distinct regimes (Table 1). The microbial mat sample off
262 Crimea is characterized by diverse uns-GDGTs with different numbers of double bonds (1-5)
263 and cyclopentyl moieties (0-2) ($GDGT_{[0-2]:[1-5]}$; Fig. 5). Although uns-GDGTs show less diversity
264 in the seep sediment off Pakistan, they dominate the archaeal IPL pool (Fig. 6). In surface
265 sediments from the two anoxic basins (Black Sea and Cariaco Basin), uns-GDGTs occur both as
266 CLs ($GDGT_{0:[1-6]}$) and IPLs (1G- and 2G-$GDGT_{0:[1-3]}$) despite being in lower relative abundance
267 than those at the seep sites (Fig. 6). Notably, we observe that sedimentary uns-GDGTs are
268 typically enriched in the reactive IPL pool (e.g., up to 98%; Fig. 6) in these samples, suggesting
269 they are largely produced by some benthic archaea, in which uns-GDGTs represent an important
270 class of lipids. By contrast, uns-GDGTs were not detected in sediments from the upwelling area

off NW Africa and were in a trace amount in the Eastern Mediterranean Sea, both of which are characterized by oxic bottom waters. Likewise, uns-GDGTs were in a trace amount in the alkaline anoxic Discovery Basin.

Although geochemical conditions vary dramatically, it appears that anoxic conditions and high fluxes of methane can stimulate the growth of selected archaea capable of synthesizing uns-GDGTs, implying a chemotaxonomic potential of uns-GDGT lipids. We tentatively suggest the following possible links of uns-GDGTs to specific archaea and the physiological role of uns-GDGTs in archaeal cytoplasmic membranes: i) methane-metabolizing archaea and/or other archaea living spatially in close association with methane-oxidizing consortia are among the sources of uns-GDGTs. Systematic investigations of environments hosting methane-oxidizing communities combined with phylogenetic and compound-specific $\delta^{13}C$ analysis will be required to substantiate this link; ii) biosynthesis of unsaturated bacterial lipids (e.g. fatty acids) fluidizes bacterial membranes [38], allowing bathypelagic bacteria to cope with low temperature and high hydrostatic pressure [39; 40]. By analogy, if uns-GDGT lipids were to fluidize archaeal membranes, it is possible that bathypelagic archaea are capable of biosynthesizing uns-GDGTs in response to environmental stress. Analysis of archaeal lipids from suspended particles in bathypelagic waters is necessary to validate this working hypothesis; iii) unsaturated bacterial lipids facilitate the transport of electron carriers (e.g., quinones) within membranes, resulting in enhanced energy production [41]. Likewise, uns-AR and uns-GDGTs may also promote energy production. We speculate that selected archaea may preferentially synthesize unsaturated ether lipids to enhance energy outputs and facilitate rapid across-membrane transport of nutrients and substances (cf. [42]). Further measurements on metabolic rate and uns-GDGT abundance in seep and non-seep

293 settings will be required to validate this potential relationship between uns-GDGT biosynthesis
294 and bioenergetics.
295
296 **Conclusions**
297 We report the discovery of several novel uns-GDGT lipids that contain between one and six
298 double bonds and zero to two cyclopentyl moieties. Identification of these lipids was achieved
299 via comparison of lipid distribution before and after hydrogenation, characteristic retention time
300 patterns, and diagnostic product ions using LC/MS, and ether cleavage products using GC/MS.
301 Isomerism resulting from various unsaturation patterns within the two biphytanyl moieties was
302 observed and specific positions of double bonds in the biphytene and biphytadiene moieties of
303 uns-GDGTs were tentatively assigned. IPL-uns-GDGTs associated with 1G, 2G, and PG
304 headgroups were also detected. Uns-GDGTs have been readily overlooked using the
305 conventional NP-LC/APCI/MS approach due to low chromatographic resolution and improper
306 conditions for ionization of these lipids. The environmental distribution of uns-GDGTs was
307 scanned using the RP-LC/ESI/MS approach in diverse marine samples. The results suggest that
308 uns-GDGTs constitute an important archaeal lipid group in euxinic basins and seep sites.
309 However, they were either undetected or in trace amounts in sediments from oxic settings and a
310 brine pool. The distribution pattern suggests that uns-GDGTs harbor chemotaxonomic
311 information and may reflect new adaptive strategies utilized by uncultivated archaea.
312
313 **5. Acknowledgements**
314 This work was funded by the Deutsche Forschungsgemeinschaft (DFG) by a postdoctoral
315 fellowship granted through the Cluster of Excellence/Research Center MARUM to C.Z., and

funded by the European Research Council under the European Union's Seventh Framework Programme–"Ideas" Specific Programme, ERC grant agreement No. 247153 (K.-U.H.). Sediment samples from the Eastern Mediterranean Sea and Discovery Basin were collected by R/V *Meteor* M84/1 (DARCSEAS), the sample off Pakistan were taken by R/V *Meteor* M74/3. We are grateful to Prof. Stuart G. Wakeham for providing the samples from the Black Sea (R/V *Knorr* 172/8) and Cariaco Basin (B/O *Hermano Gines* CAR139), Prof. Gesine Mollenhauer for the sample off NW Africa (R/V *Maria S. Merian* 11/2), and Dr. Florence Schubotz (R/V *Meteor* M72/2) for the mat sample off Crimea. We thank all participating scientists and ship crews for sample recovery. We also thank three anonymous reviewers for their thoughtful comments.

6. References

1.Schouten S., Hopmans E.C., Schefuss E., Sinninghe Damsté J.S. Distributional variations in marine crenarchaeotal membrane lipids: a new tool for reconstructing ancient sea water temperatures? *Earth Planet. Sci. Lett.* **2002**, 204, 265-274.

2.Shimada H., Nemoto N., Shida Y., Oshima T., Yamagishi A. Effects of pH and temperature on the composition of polar lipids in *Thermoplasma acidophilum HO-62*. *J. Bacteriol.* **2008**, 190, 5404-5411.

3.Gibson J.A.E., Miller M.R., Davies N.W., Neill G.P., Nichols D.S., Volkman J.K. Unsaturated diether lipids in the psychrotrophic archaeon Halorubrum lacusprofundi. *Syst. Appl. Microbiol.* **2005**, 28, 19-26.

4.Dawson K.S., Freeman K.H., Macalady J.L. Molecular characterization of core lipids from halophilic archaea grown under different salinity conditions. *Org. Geochem.* **2012**, 48, 1-8.

5.Hafenbradl D., Keller M., Thiericke R., Stetter K.O. A novel unsaturated archaeal ether core lipid from the hyperthermophile *methanopyrus-kandleri*. *Syst. Appl. Microbiol.* 1993, 16, 165-169.

6.Maestrojuan G.M., Boone J.E., Mah R.A., Menaia J.A.G.F., Sachs M.S., Boone D.R. Taxonomy and halotolerance of mesophilic methanosarcina strains, assignment of strains to species, and synonymy of *methanosarcina-mazei* and *Methanosarcina-frisia*. *Int. J. Syst. Bacteriol.***1992**, 42, 561-567.

7.Schouten S., Vandermaarel M.J.E.C., Huber R., Damste J.S.S. 2,6,10,15,19-Pentamethylicosenes in Methanolobus bombayensis, a marine methanogenic archaeon, and in Methanosarcina mazei. *Org. Geochem.* **1997**, 26, 409-414.

8.Elvert M., Suess E., Whiticar M.J. Anaerobic methane oxidation associated with marine gas hydrates: superlight C-isotopes from saturated and unsaturated C-20 and C-25 irregular isoprenoids. *Naturwissenschaften,* **1999**, 86, 295-300.

9.Orphan V.J., Hinrichs K.U., Ussler W., Paull C.K., Taylor L.T., Sylva S.P., Hayes J.M., Delong E.F. Comparative analysis of methane-oxidizing archaea and sulfate-reducing bacteria in anoxic marine sediments. *Appl. Environ. Microbiol.* **2001**, 67, 1922-1934.

10.Blumenberg M., Seifert R., Reitner J., Pape T., Michaelis W. Membrane lipid patterns typify distinct anaerobic methanotrophic consortia. *Proc. Natl. Acad. Sci. U.S.A.* **2004**, 101, 11111-11116.

11.Niemann H., Elvert M. Diagnostic lipid biomarker and stable carbon isotope signatures of microbial communities mediating the anaerobic oxidation of methane with sulphate. *Org. Geochem.* **2008**, 39, 1668-1677.

12.Franzmann P.D., Stackebrandt E., Sanderson K., Volkman J.K., Cameron D.E., Stevenson P.L., Mcmeekin T.A., Burton H.R. *Halobacterium-lacusprofundi Sp-Nov*, a halophilic bacterium Isolated from deep lake, Antarctica. *Syst. Appl. Microbiol.* **1988**, 11, 20-27.

13.Nichols P.D., Franzmann P.D. Unsaturated Diether Phospholipids in the Antarctic Methanogen Methanococcoides-Burtonii. *Fems Microbiol. Lett,* **1992**, 98, 205-208.

14.Nichols D.S., Miller M.R., Davies N.W., Goodchild A., Raftery M., Cavicchioli R. Cold adaptation in the antarctic archaeon *Methanococcoides burtonii* involves membrane lipid unsaturation. *J. Bacteriol.* **2004**, 186, 8508-8515.

15.Morii H., Eguchi T., Nishihara M., Kakinuma K., Konig H., Koga Y. A novel ether core lipid with H-shaped C-80-isoprenoid hydrocarbon chain from the hyperthermophilic methanogen *Methanothermus fervidus*. *Biochim. Biophys. Acta.* **1998**, 1390, 339-345.

16.Boyd E.S., Pearson A., Pi Y.D., Li W.J., Zhang Y.G., He L., Zhang C.L., Geesey G.G. Temperature and pH controls on glycerol dibiphytanyl glycerol tetraether lipid composition in the hyperthermophilic crenarchaeon *Acidilobus sulfurireducens*. *Extremophiles* **2011**, 15, 59-65.

17.Huguet C., Fietz S., Rosell-Mele A. Global distribution patterns of hydroxy glycerol dialkyl glycerol tetraethers. *Org. Geochem.* **2013**, 57, 107-118.

18.Zhu C., Lipp J.S., Wormer L., Becker K.W., Schroder J., Hinrichs K.U. Comprehensive glycerol ether lipid fingerprints through a novel reversed phase liquid chromatography-mass spectrometry protocol. *Org. Geochem.* **2013**, 65, 53-62.

19. Michaelis W., Seifert R., Nauhaus K., Treude T., Thiel V., Blumenberg M., Knittel K., Gieseke A., Peterknecht K., Pape T., Boetius A., Amann R., Jorgensen B.B., Widdel F., Peckmann J., Pimenov N.V., Gulin M.B. Microbial reefs in the Black Sea fueled by anaerobic oxidation of methane. *Science* **2002**, 297, 1013-1015.

20. Fischer D., Sahling H., Nothen K., Bohrmann G., Zabel M., Kasten S. Interaction between hydrocarbon seepage, chemosynthetic communities, and bottom water redox at cold seeps of the Makran accretionary prism: insights from habitat-specific pore water sampling and modeling. *Biogeosciences* **2012**, 9, 2013-2031.

21. Wakeham S.G., Hopmans E.C., Schouten S., Damste J.S.S. Archaeal lipids and anaerobic oxidation of methane in euxinic water columns: a comparative study of the Black Sea and Cariaco Basin. *Chem. Geol.* **2004**, 205, 427-442.

22. Bethoux J.P. Oxygen-Consumption, New Production, Vertical Advection and Environmental Evolution in the Mediterranean-Sea. *Deep-Sea Res.* **1989**, 36, 769-781.

23. Van Der Wielen P.W.J.J., Bolhuis H., Borin S., Daffonchio D., Corselli C., Giuliano L., D'auria G., De Lange G.J., Huebner A., Varnavas S.P., Thomson J., Tamburini C., Marty D., Mcgenity T.J., Timmis K.N., Party B.S. The enigma of prokaryotic life in deep hypersaline anoxic basins. *Science* **2005**, 307, 121-123.

24. Sturt H.F., Summons R.E., Smith K., Elvert M., Hinrichs K.U. Intact polar membrane lipids in prokaryotes and sediments deciphered by high-performance liquid chromatography/electrospray ionization multistage mass spectrometry - new biomarkers for biogeochemistry and microbial ecology. *Rapid Commun. Mass Spectrom.* **2004**, 18, 617-628.

25. Pancost R.D., Bouloubassi I., Aloisi G., Damste J.S.S., Party M.S.S. Three series of non-isoprenoidal dialkyl glycerol diethers in cold-seep carbonate crusts. *Org. Geochem.* **2001**, 32, 695-707.

26. Biddle J.F., Lipp J.S., Lever M.A., Lloyd K.G., Sorensen K.B., Anderson R., Fredricks H.F., Elvert M., Kelly T.J., Schrag D.P., Sogin M.L., Brenchley J.E., Teske A., House C.H., Hinrichs K.U. Heterotrophic Archaea dominate sedimentary subsurface ecosystems off Peru. *Proc. Natl. Acad. Sci. U.S.A.* **2006**, 103, 3846-3851.

27. Jahnke L.L., Orphan V.J., Embaye T., Turk K.A., Kubo M.D., Summons R.E., Des Marais D.J. Lipid biomarker and phylogenetic analyses to reveal archaeal biodiversity and distribution in hypersaline microbial mat and underlying sediment. *Geobiology* **2008**, 6, 394-410.

28. Schouten S., Huguet C., Hopmans E.C., Kienhuis M.V.M., Sinninghe Damsté J.S. Analytical methodology for TEX_{86} paleothermometry by high-performance liquid chromatography/atmospheric pressure chemical ionization-mass spectrometry. *Anal. Chem.* **2007**, 79, 2940-2944.

29. Cook H.W., Mcmaster C.R. Fatty acid desaturation and chain elongation in eukaryotes, Vance D. E. and Vance J.E. (Eds.) Biochemistry of lipid, lipoproteins and membrane (4th Edn.). **2002**, Chapter 7.

30. Knappy C.S., Chong J.P.J., Keely B.J. Rapid discrimination of archaeal tetraether lipid cores by liquid chromatography-tandem mass spectrometry. *J. Am. Soc. Mass. Spectrom.* **2009**, 20, 51-59.

31. Yoshinaga M.Y., Kellermann M.Y., Rossel P.E., Schubotz F., Lipp J.S., Hinrichs K.U. Systematic fragmentation patterns of archaeal intact polar lipids by high-performance liquid chromatography/electrospray ionization ion-trap mass spectrometry. *Rapid Commun. Mass Spectrom.* **2011**, 25, 3563-3574.

32. Becker K.W., Lipp J.S., Zhu C., Liu X.L., Hinrichs K.U. An improved method for the analysis of archaeal and bacterial ether core lipids. *Org. Geochem.* **2013**, 61, 34-44.

33. Schouten S., Hoefs M.J.L., Koopmans M.P., Bosch H.J., Damste J.S.S. Structural characterization, occurrence and fate of archaeal ether-bound acyclic and cyclic biphytanes and corresponding diols in sediments. *Org. Geochem.* **1998**, 29, 1305-1319.

34. Risatti J.B., Rowland S.J., Yon D.A., Maxwell J.R. Stereochemical studies of acyclic isoprenoids. XII. Lipids of methanogenic bacteria and possible contributions to sediments. *Org. Geochem.* **1984**, 6, 93-104.

35. Elvert M., Suess E., Greinert J., Whiticar M.J. Archaea mediating anaerobic methane oxidation in deep-sea sediments at cold seeps of the eastern Aleutian subduction zone. *Org. Geochem.* **2000**, 31, 1175-1187.

36. Nishihara M., Morii H., Matsuno K., Ohga M., Stetter K.O., Koga Y. Structural analysis by reductive cleavage with LiAlH4 of an allyl ether choline-phospholipid, archaetidylcholine, from the hyperthermophilic methanoarchaeon Methanopyrus kandleri. *Archaea* **2002**, 1, 123-131.

37. Zhang Y.G., Zhang C.L.L., Liu X.L., Li L., Hinrichs K.U., Noakes J.E. Methane Index: A tetraether archaeal lipid biomarker indicator for detecting the instability of marine gas hydrates. *Earth Planet. Sci. Lett.* **2011**, 307, 525-534.

38. Cronan J.E., Gelmann E.P. Physical-properties of membrane lipids - biological relevance and regulation. *Bacteriol. Rev.* **1975**, 39, 232-256.

39. Delong E.F., Yayanos A.A. Adaptation of the membrane-lipids of a deep-sea bacterium to changes in hydrostatic-pressure. *Science* **1985**, 228, 1101-1102.

40. Fang J.S., Chan O.V., Kato C., Sato T., Peeples T., Niggemeyer K. Phospholipid FA of piezophilic bacteria from the deep sea. *Lipids* **2003** 38, 885-887.

41. Valentine R.C., Valentine D.L. Omega-3 fatty acids in cellular membranes: a unified concept. *Prog. Lipid Res.* **2004**, 43, 383-402.

42. Yoshinaga M.Y., Wormer L., Elvert M., Hinrichs K.U. Novel cardiolipins from uncultured methane-metabolizing archaea. *Archaea* **2012**, http://dx.doi.org/10.1155/2012/832097.

Figure captions

Fig. 1. Partial extracted ion chromatograms of tetraether lipids (detected as $[M+NH_4]^+$) from a cold seep sediment (6-8 cm) off Pakistan before (A) and after (B) hydrogenation analyzed by RP-ESI-MS_{MSD}, and the relative abundances (normalized to cren) before and after hydrogenation (C). The box shows vertically enlarged peaks of compounds **V**-**VII.** cren = crenarchaeol, cren' = crenarchaeol regioisomer. Unsaturated GDGTs are expressed as GDGT*n*:*m*, where *n* = the number of cyclopentyl moieties, and *m* = the number of double bonds.

Fig. 2. MS^2 spectra of compounds **I** ($[GDGT_{0:1} + NH_4]^+$; *m/z* 1317)**, II** ($[GDGT_{0:2} + NH_4]^+$; *m/z* 1315)**,** and **III** ($[GDGT_{0:3} + NH_4]^+$; *m/z* 1313) (cf. Fig. 1) from a cold seep sediment (6-8 cm) off Pakistan obtained by RP-LC/ESI/MS_{qTOF} (A), and the GC-MS spectra of highest concentrated biphytene and biphytadiene cleaved from 2G-uns-GDGTs from the same sample (B). Diamonds in panel A indicate the ammoniated precursor molecules $[M+NH_4]^+$. The insert in right panel B shows the total ion chromatogram of major biphytanes/biphytenes/biphytadienes after ether cleavage; for peaks labeled with *, their detailed mass spectra are shown. Note, that the assignment of double bond positions in $BP_{0:1}$ and $BP_{0:2}$ is tentative, one double bond is likely located at C-3 and the other likely between C-7 and C-15 (dashed lines; also see text).

Fig. 3. Partial composite mass chromatograms of 1G-GDGTs (A), 2G-GDGTs (B), and PG-GDGTs (C) from a cold seep sediment (6-8 cm) off Pakistan obtained by RP-LC/ESI/MS_{MSD}. Legends: 0-3, cren, and cren' denote the core lipid moieties of $GDGT_{0-3}$, crenarchaeol, and crenarchaeol regioisomer, respectively; mono, di, and tri indicate core lipid moieties of

518 $GDGT_{0:[1-3]}$, respectively; 1G = mono-glycosyl; 2G = di-glycosyl; and PG =
519 phosphatidylglycerol.
520
521 **Fig. 4**. Partial composite mass chromatograms of archaeal GDGTs from a cold seep sediment (6-
522 8 cm) off Pakistan detected by RP-LC/ESI/MS_{MSD} (A), NP-LC/APCI/MS_{MSD} (B), NP-
523 LC/ESI/MS_{MSD} (C), and comparison of the methane index (MI) values determined by all three
524 approaches (D). Core lipids were detected as $[M+NH_4]^+$ after ESI and $[M+H]^+$ after APCI.
525 Labels **I-III**, cren, and cren' are the same as in Fig.1; numbers 0-4 denote $GDGT_{0-4}$, respectively;
526 peaks **1+I**, **2+II**, and **3+III** indicate co-elution of isobaric uns-$GDGT_{0:[1-3]}$ and cyclic $GDGT_{1-3}$.
527 The insert in panel B shows a partial mass spectrum of peak **2+II** obtained by NP-
528 LC/APCI/MS_{MSD} in full scan mode.
529
530 **Fig. 5**. Partial extracted ion $[M+NH_4]^+$ chromatograms of archaeal GDGTs from a microbial mat
531 sample in the Black Sea off Crimea analyzed by RP-LC/ESI/MS_{MSD}. Unsaturated GDGTs are
532 expressed as GDGT*n*:*m*, where *n* = the number of cyclopentyl moieties, and *m* = the number of
533 double bonds.
534
535 **Fig. 6**. The unsaturated fractions (%) in three classes of archaeal IPLs (defined by 1G, 2G, and
536 PG headgroups) and corresponding core lipids from seven depositional settings. Legends: BS =
537 Black Sea; CB = Cariaco Basin; PM = cold seep off Pakistan; EMS = Eastern Mediterranean Sea;
538 NWA = upwelling off NW Africa; DB = Discovery Basin; MAT = microbial mat sample from a
539 Crimean seep. 1G, 2G, and PG refer to Fig. 4.
540

541 **Table 1**. Marine sediment and microbial mat samples obtained from various depositional settings.

Area	Cold seep off Pakistan	Black Sea	Cariaco Basin	Eastern Mediterranean Sea	Upwelling Area - NW Africa	Discovery Basin	Off Crimea, Ghostdabs field
Code	PA	BC	CB	EMS	NWA	DB	MAT
Water redox	core of oxygen minimum zone	anoxic basin	anoxic basin	oligotrophic, oxic	upwelling, oxic	Hypersaline, anoxic	anoxic
Cruise	R/V *Meteor* 74/3	R/V *Knorr* 172/8	B/O *Hermano Gines* CAR139	R/V *Meteor* 84/1	R/V *Maria S. Merian* 11/2	R/V *Meteor* 84/1	R/V *Meteor* 72/2
Core/Station	GeoB 12320	BS5-4BC	CARIACO	GeoB 15103	GeoB 13612	GeoB 15102	Station 322
Water depth	550 m	2190 m	1400 m	1367 m	2690 m	3615 m	300 m
Position	24°53'N 63°01'E	43°N 34°E	10°40'N 65°36'W	32°38'N 34°01'E	20°47'N 18°44'W	35°16'N 21°42'E	44°46'N 31°55'E
Sediment depth	6-8 cm	0-3 cm	0-10 cm	10-12 cm	0-1 cm	0-2 cm	chimney-derived microbial mat
TOC	2.2%	2.7%	3.0%	1.3%	2.1%	0.13%	/
Lipid extraction	Modified Bligh and Dyer	Soxhlet	Soxhlet	Modified Bligh and Dyer	Soxhlet	Modified Bligh and Dyer	Modified Bligh and Dyer

542

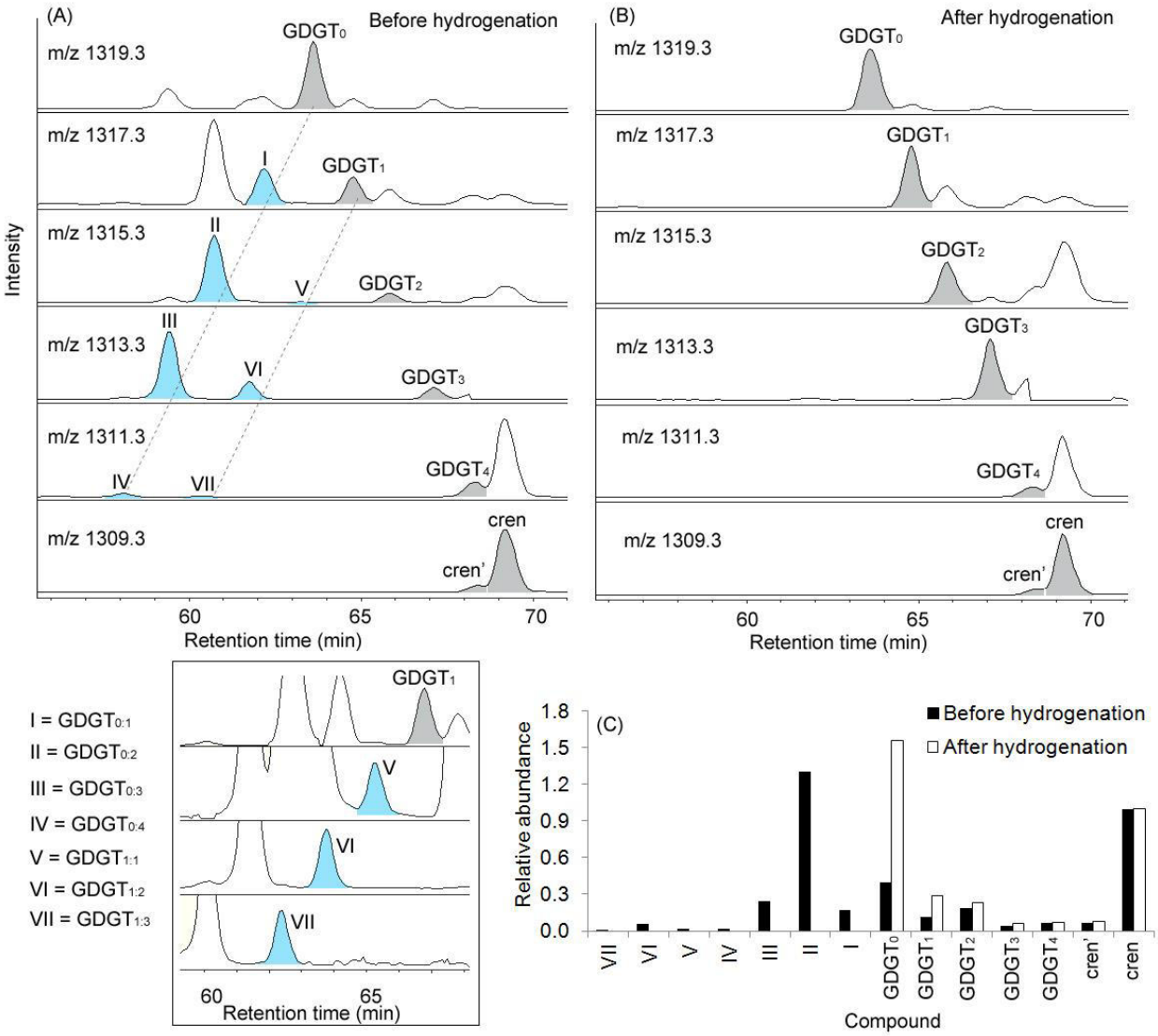
(A)
Before hydrogenation
(B)
After hydrogenation
m/z 1319.3
m/z 1317.3
m/z 1315.3
m/z 1313.3
m/z 1311.3
m/z 1309.3
GDGT0
GDGT1
GDGT2
GDGT3
GDGT4
I
II
III
IV
V
VI
VII
cren
cren'
Intensity
Retention time (min)
60
65
70
I = GDGT0:1
II = GDGT0:2
III = GDGT0:3
IV = GDGT0:4
V = GDGT1:1
VI = GDGT1:2
VII = GDGT1:3
(C)
Before hydrogenation
After hydrogenation
Relative abundance
Compound
0.0
0.3
0.6
0.9
1.2
1.5
1.8

Fig. 1.

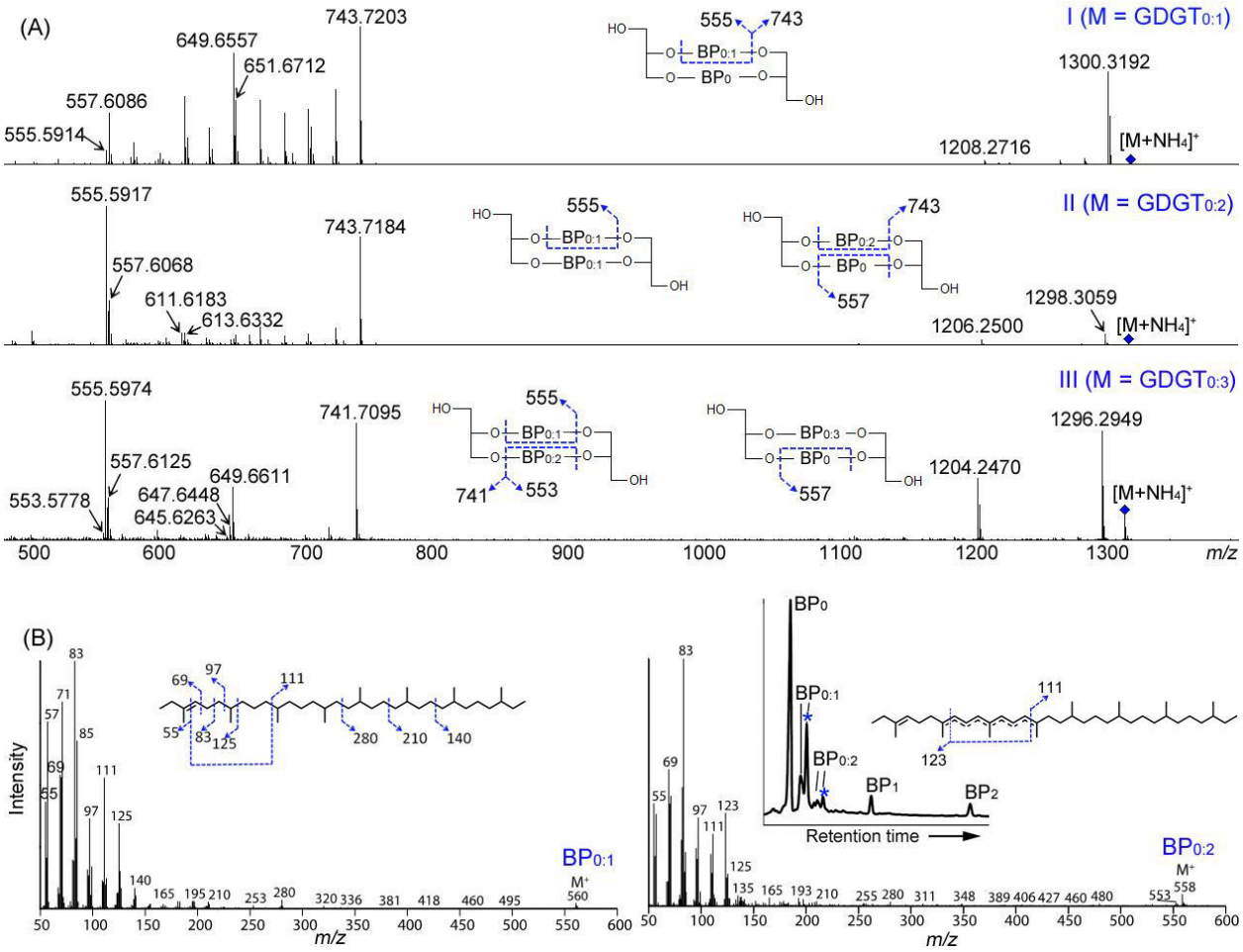
(A)
I (M = GDGT0:1)
II (M = GDGT0:2)
III (M = GDGT0:3)
[M+NH4]+
m/z
(B)
Intensity
BP0:1
BP0:2
BP0
BP1
BP2
Retention time
M+

Fig. 2.

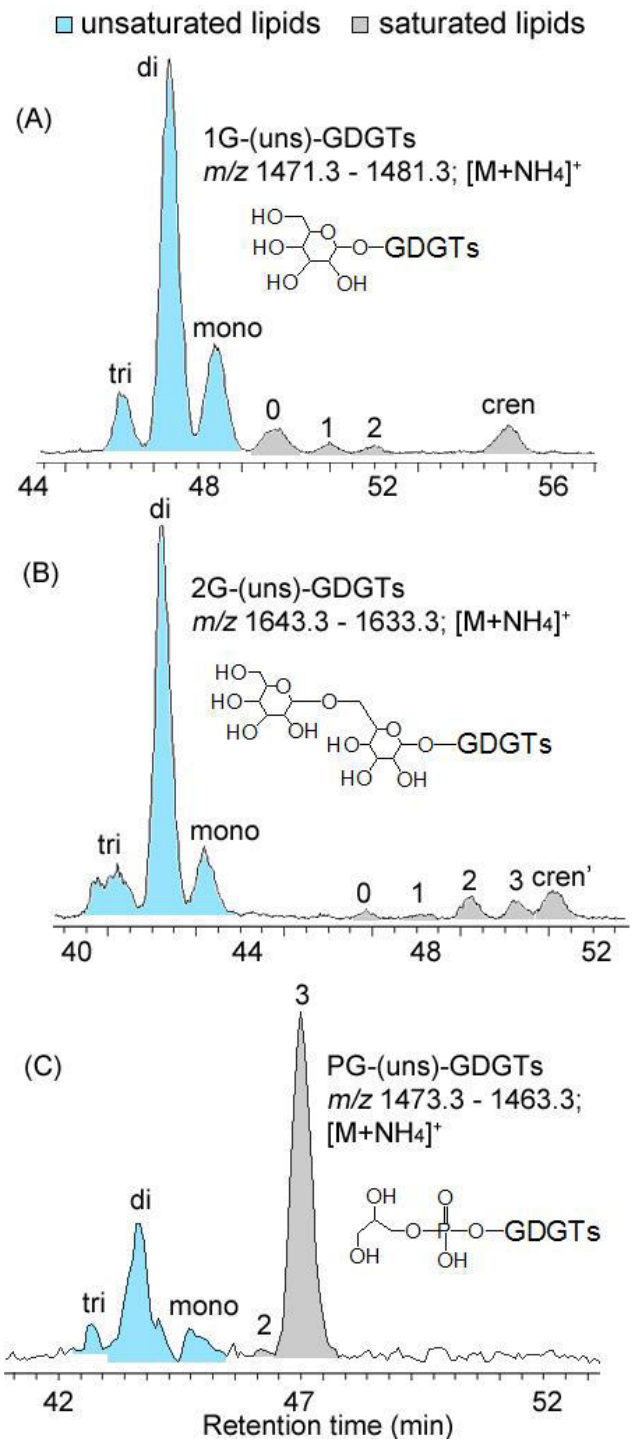
unsaturated lipids
saturated lipids
(A)
1G-(uns)-GDGTs
m/z 1471.3 - 1481.3; [M+NH4]+
HO
HO
HO
O
O—GDGTs
OH
di
mono
tri
0
1
2
cren
44
48
52
56
(B)
2G-(uns)-GDGTs
m/z 1643.3 - 1633.3; [M+NH4]+
HO
HO
HO
OH
O
O—GDGTs
di
mono
tri
0
1
2
3
cren'
40
44
48
52
(C)
PG-(uns)-GDGTs
m/z 1473.3 - 1463.3;
[M+NH4]+
OH
O
O
P
O—GDGTs
OH
OH
3
di
tri
mono
2
42
47
52
Retention time (min)

Fig. 3.

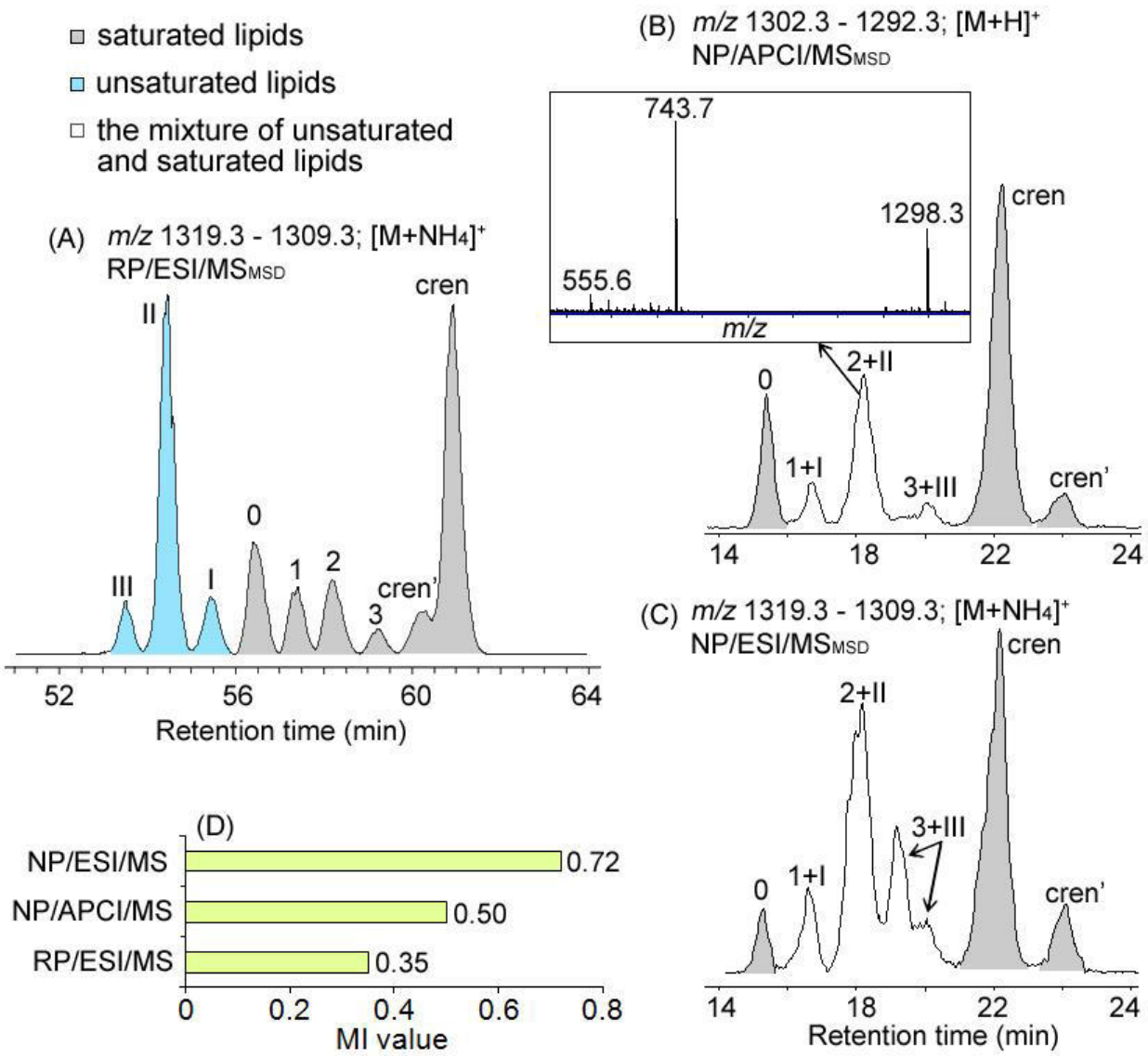
saturated lipids
unsaturated lipids
the mixture of unsaturated and saturated lipids
(A) m/z 1319.3 - 1309.3; [M+NH4]+
RP/ESI/MSMSD
II
III
I
0
1
2
3
cren
cren'
52
56
60
64
Retention time (min)
(B) m/z 1302.3 - 1292.3; [M+H]+
NP/APCI/MSMSD
743.7
1298.3
555.6
m/z
0
2+II
1+I
3+III
cren
cren'
14
18
22
24
(C) m/z 1319.3 - 1309.3; [M+NH4]+
NP/ESI/MSMSD
0
1+I
2+II
3+III
cren
cren'
14
18
22
24
Retention time (min)
(D)
NP/ESI/MS
NP/APCI/MS
RP/ESI/MS
0.72
0.50
0.35
0
0.2
0.4
0.6
0.8
MI value

Fig. 4.

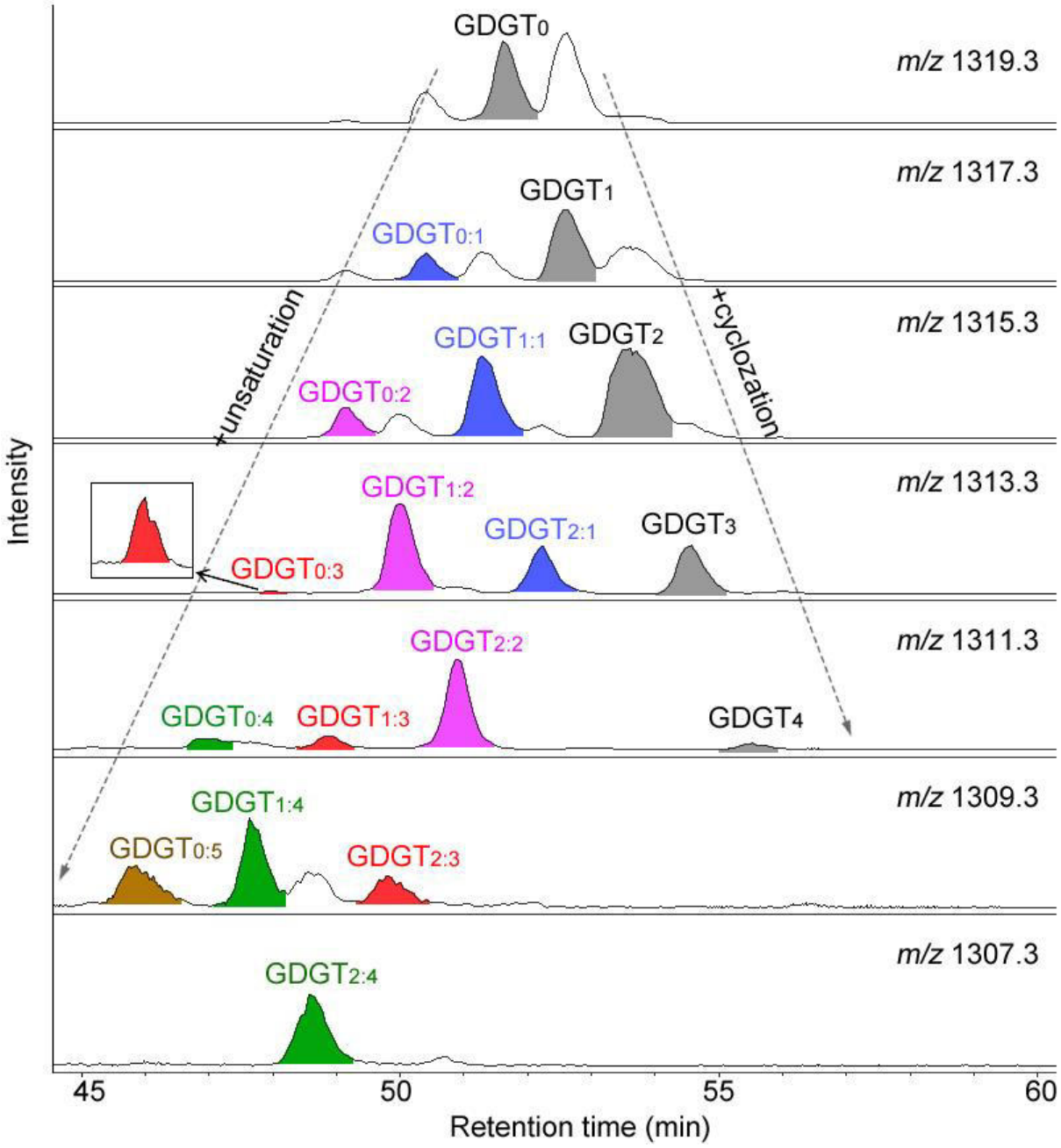
GDGT0
m/z 1319.3
GDGT1
GDGT0:1
m/z 1317.3
+unsaturation
+cyclozation
GDGT1:1
GDGT2
GDGT0:2
m/z 1315.3
GDGT1:2
GDGT2:1
GDGT3
GDGT0:3
m/z 1313.3
GDGT2:2
GDGT0:4
GDGT1:3
GDGT4
m/z 1311.3
GDGT1:4
GDGT0:5
GDGT2:3
m/z 1309.3
GDGT2:4
m/z 1307.3
Intensity
45
50
55
60
Retention time (min)

Fig. 5.

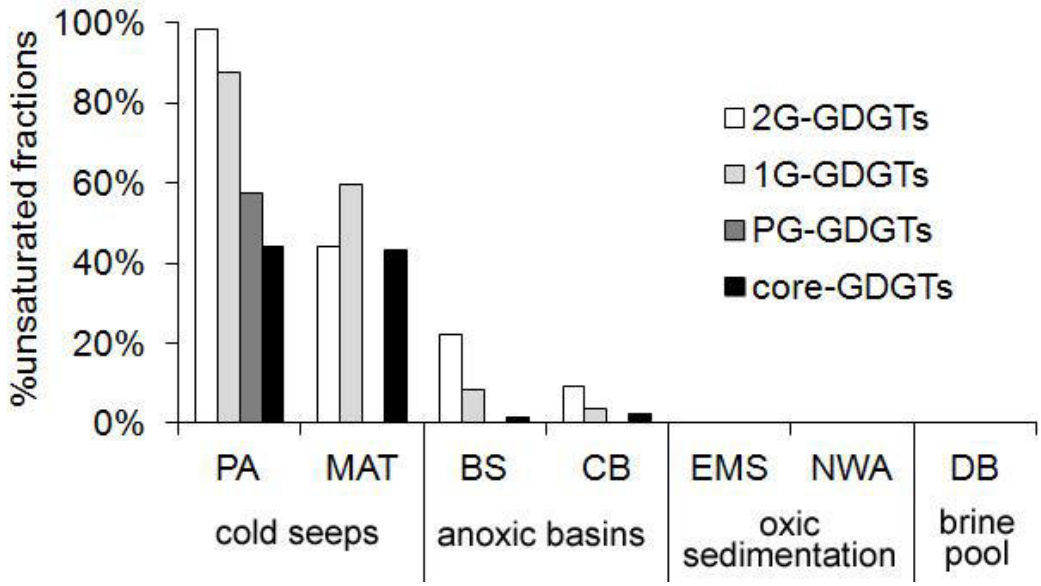
%unsaturated fractions
100%
80%
60%
40%
20%
0%
2G-GDGTs
1G-GDGTs
PG-GDGTs
core-GDGTs
PA
MAT
BS
CB
EMS
NWA
DB
cold seeps
anoxic basins
oxic sedimentation
brine pool

Fig. 6.